



# Design, Synthesis, *In silico*, *In vivo* Evaluation of 2(4-amino phenyl), 5-substituted phenyl) 1,3,4-Oxadiazoles as Potential Nootropic Agents

Suvarna A. Katti<sup>1</sup>, Manisha A. Tayde \*<sup>2</sup>, Anuja P. Bhosale<sup>3</sup>

<sup>1,3</sup> Department of Pharmaceutical Chemistry, M.G. V's Pharmacy College, Panchavati, Nasik-03

<sup>2</sup> Department of Pharmaceutical Chemistry, SPES Smt. Narmadaben Popatlal Thakkar Institute of Pharmacy, Nashik-03

(Received: 16 January 2026

Revised: 25 February 2026

Accepted: 30 March 2026)

## KEYWORDS

Alzheimer's,  
Nootropic agents,  
1,3,4-oxadiazole  
derivatives,  
Acetylcholinesterase  
inhibition, Molecular  
docking.

## ABSTRACT:

**Introduction:** Alzheimer's disease is a degenerative neurological condition marked by cognitive deterioration and memory deficit, for which effective and safe therapeutic options remain limited.

**Objective:** This study was undertaken to design, synthesize, and evaluate some designed novel oxadiazole derivatives as potential nootropic agents.

**Methodology:** A library of eighteen novel compounds was rationally designed and initially screened using in-silico tools, including PASS online tool, Swiss ADME, Pro Tox-III, and molecular docking using Molsoft ICM-Pro to assess binding affinity toward acetylcholinesterase. Based on favorable in-silico results, ten compounds were synthesized and characterized by IR and <sup>1</sup>H-NMR spectroscopy, and their purity was confirmed by HPTLC analysis.

**Results:** Molecular docking studies publicized that numerous compounds exhibited robust binding affinity toward acetylcholinesterase, with docking scores comparable to or superior to the standard nootropic drug Piracetam. Among the synthesized derivatives, PS-1, PS-11, and PS-14 demonstrated optimal pharmacokinetic properties, blood-brain barrier permeability, and acceptable safety profiles. These compounds were further evaluated for nootropic activity using scopolamine-induced amnesia models in mice, namely the Elevated Plus Maze and Morris Water Maze.

**Discussion:** The finding showed that PS-1, PS-11, PS-14 produced a significant improvement in learning and memory parameters in a dose-dependent manner, equivalent to Piracetam. Particularly PS-14, represent promising lead candidates for the discovery of novel nootropic agents.

**Conclusion:** The strong correlation between in-silico predictions and in-vivo outcomes validates the rational design strategy and supports further investigation of these compounds for the treatment of cognitive diseases, including Alzheimer's disease.

## 1. Introduction

Alzheimer's disease (AD) is the predominant and progressive form of dementia, representing a major global health challenge due to its irreversible nature and increasing prevalence [1-3]. Pathologically, AD is characterized by the presence of extracellular neuritic plaques and intracellular neurofibrillary tangles, that disrupts standard neural communication and ultimately result in neuronal demise [4-5]. These pathological hallmarks primarily result from the abnormal accumulation of amyloid- $\beta$  (A $\beta$ ) peptides within the medial temporal lobe along with neocortical area of the

brain, areas critically involved in learning and memory functions [6-7].

The lack of disease-modifying therapies, coupled with the limited efficacy and adverse effects of existing treatments, underscores the imperative need for the discovery and development of novel therapeutic molecules capable of improving cognitive function and slowing disease progression [8-9]. In this context, nootropic agents, particularly those targeting cholinergic neurotransmission, have attracted significant attention for the symptomatic management of AD [10-11].



AD occurs in two major forms: sporadic AD, which constitutes the predominant share of cases and is associated with aging and environmental factors, and familial AD, a rare inherited form linked to genetic mutations [12-13].

One of the most widely accepted mechanisms is the amyloid cascade hypothesis, which suggests that abnormal managing of amyloid precursor protein leads to excessive accumulation of peptides (especially amyloid- $\beta$ ) in the brain parenchyma and cerebral vasculature. These peptides aggregate to create insoluble plaques that trigger a sequence of neurotoxic occurrences, including oxidative stress, neuroinflammation, synaptic dysfunction, and neuronal loss [14-16].

According to the Tau hyperphosphorylation hypothesis, abnormal phosphorylation of Tau proteins disrupts microtubule stability, impairing axonal transport and neuronal integrity. Neurofibrillary tangles formed by aggregated Tau proteins are strongly correlated with disease severity and cognitive decline. Tau pathology has been consistently observed in post-mortem brain tissues of patients with Alzheimer's disease, further supporting its role in disease progression [17-19].

In addition to amyloid and Tau pathology, AD is associated with extensive neuronal loss, specifically in brain areas responsible for memory, learning, and higher cognitive functions. Under normal physiological conditions, mature neurons employ sophisticated protective mechanisms to prevent activation of programmed cell fatality pathways. However, in Alzheimer's disease, these protective mechanisms become compromised, leading to the abnormal activation of many modalities of regulated cellular demise, encompassing apoptosis

and other degenerative processes. The cumulative effect of these pathological mechanisms results in progressive cognitive deterioration and functional disability [20-22].

The cholinergic hypothesis of AD proposes that cognitive impairment results primarily from a deficiency of acetylcholine in the brain. This neurotransmitter plays a critical role in learning, memory, and attention. Consequently, acetylcholinesterase inhibitors have become the cornerstone of symptomatic treatment for

AD, as they prevent the breakdown of acetylcholine and enhance cholinergic neurotransmission [23-25].

Oxadiazoles are 5-membered heterocyclic compounds containing one oxygen (O) atom and two nitrogen (N) atoms within the ring structure. Several oxadiazole derivatives have demonstrated a broad spectrum of pharmacological actions, encompassing antibacterial and anti-inflammatory properties, antitumor, anticonvulsant, and neuroprotective effects [26-29].

Piracetam (2-oxo-1-pyrrolidone-acetamide) is one of the earliest and most extensively studied nootropic agents. It is known to enhance learning and memory while minimizing cognitive impairment. The nootropic mechanism of piracetam involves multiple pathways, including reduction of acetylcholinesterase activity, attenuation of neuroinflammatory mediators, suppression of pro-apoptotic proteins, and mitigation of oxidative stress within the cerebral environment [30-31].

The present research work is a continuation of our earlier studies involving the synthesis of 1,2,4-oxadiazole derivatives and evaluated for nootropic activity [32]. Building upon these findings, the current investigation aims to explore 2-(4-aminophenyl), 5-substituted phenyl-1,3,4-oxadiazoles as potential nootropic agents through systematic design, synthesis, in-silico docking, and in-vivo pharmacological evaluation. The outcomes of this study are expected to provide valuable insights into SAR and contribute to the advancement of novel therapeutic candidates for the management of AD.

## 2. Objectives

The present research work is a continuation of our earlier studies involving the synthesis of 1,2,4-oxadiazole derivatives and evaluated for nootropic activity [32]. Building upon these findings, the current investigation aims to explore 2-(4-aminophenyl), 5-substituted phenyl-1,3,4-oxadiazoles as potential nootropic agents through systematic design, synthesis, in-silico docking, and in-vivo pharmacological evaluation. The outcomes of this study are expected to provide valuable insights into SAR and contribute to the advancement of novel therapeutic candidates for the management of AD.



### 3. Methods

#### 3.1 Design library of compounds

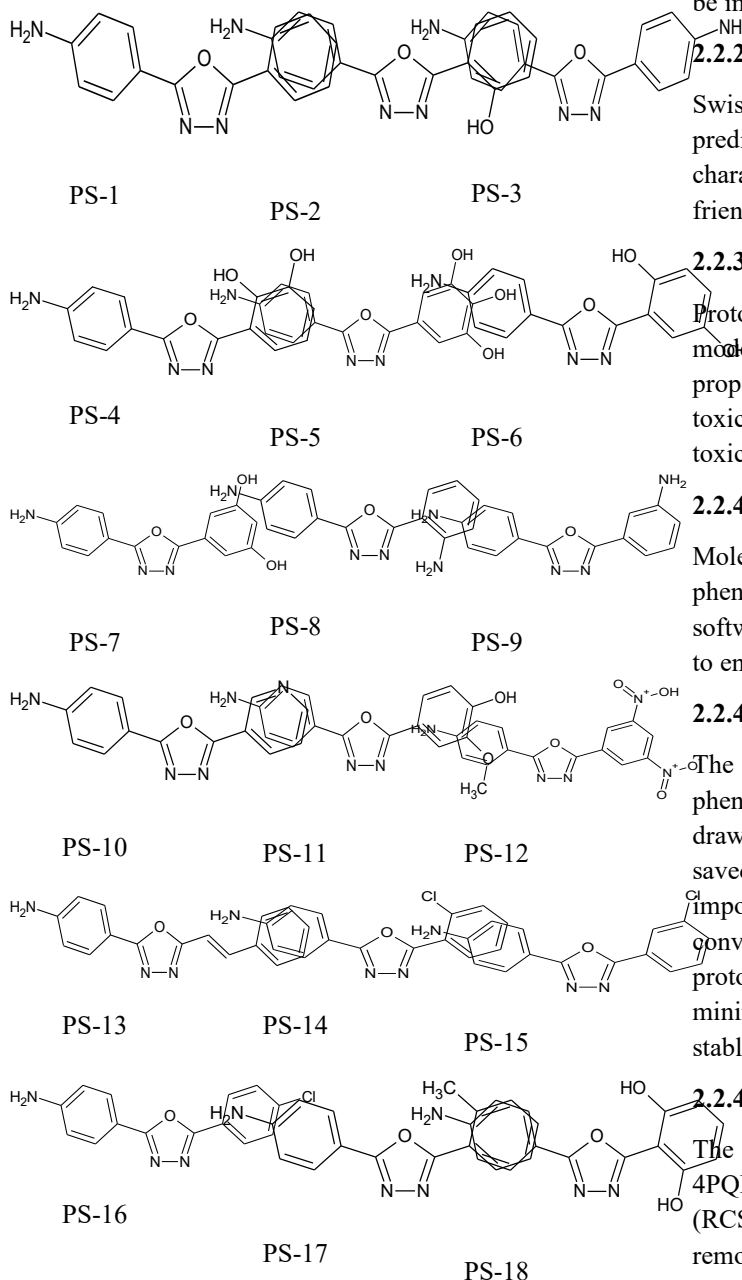


Figure1. Design of Library of compounds

#### 2.2 In-silico Evaluation of Designed Compounds

##### 2.2.1 Biological Activity

PASS ("Prediction of Activity Spectra for Substances") is computer-aided software program. In this probability that the predicted compound falls into the category of active compounds is assessed by Pa (probability "to be

active"), and the probability of falling into the category of inactive compounds is assessed as Pi (probability "to be inactive")<sup>[33]</sup>.

##### 2.2.2 Pharmacokinetic properties

Swiss ADME a computer-aided software was utilized to predict pharmacokinetics, physicochemical characteristics, drug likeness, and medicinal chemistry friendliness properties of designed compounds<sup>[34]</sup>.

##### 2.2.3 Toxicity Studies

Protox III software which utilizes machine learning models, pharmacophore-based approaches, fragment propensities, and molecular similarity to predict various toxicity endpoints was utilized to predicts multiple toxicity levels<sup>[35]</sup>.

##### 2.2.4 Molecular docking

Molecular docking of 2(4-amino phenyl),5- substituted phenyl) 1,3,4- oxadiazoles was performed using Molsoft software to examine mechanisms by which ligand bind to enzyme Acetyl Choline esterases<sup>[36]</sup>.

##### 2.2.4.1 Ligand Preparation

The chemical structures of the designed 2(4-amino phenyl),5- substituted phenyl) 1,3,4-oxadiazoles were drawn using ACD/ChemSketch, and the structures were saved as mol format. These 2D structures were then imported into Molsoft ICM-Pro, where they were converted into 3D conformations. Each ligand was protonated at physiological pH 7.4 and energy minimized utilizing the MMFF94 force field to obtain a stable and low-energy structure suitable for docking.

##### 2.2.4.2 Protein Preparation

The crystal structure of acetylcholinesterase (PDB ID: 4PQE) was taken from webserver Protein Data Bank (RCSB). The protein was prepared in ICM-Pro by removing water molecules, correcting any missing side chains or atoms, and adding hydrogen atoms. The structure was then minimized to remove any strain in the structure. From the position of the co-crystallized ligand the active site was identified<sup>[37]</sup>. Molecular docking was done using the flexible docking algorithm of Molsoft ICM-Pro<sup>[38]</sup>.

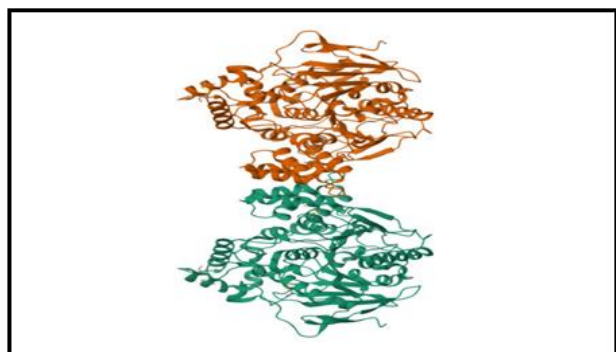
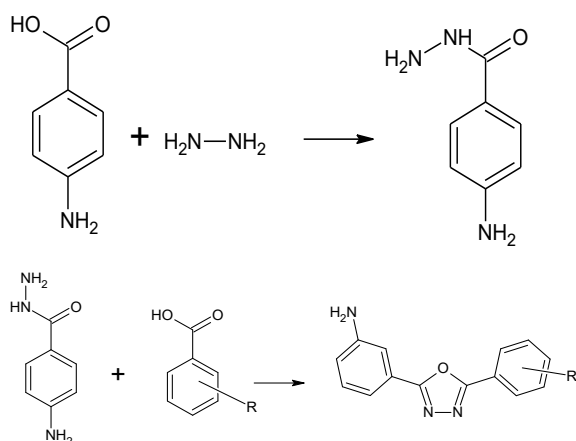


**Figure 2.** Crystal Structure of PDB id: 4PQE (Human Acetylcholinesterase)

Acetylcholinesterase was found to interact with designed molecules through key regions such as the active site (Ser203, His447 and Glu334), anionic site (Trp86, Tyr133, Glu202), acyl binding site (Trp236, Phe295, Phe297), and oxyanion site (Gly121, Gly122). Notably, TRP286 was found to be essential for ligand binding and inhibition of enzyme activity<sup>[39-40]</sup>.

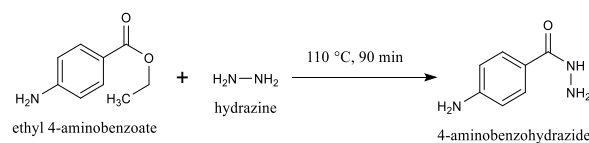
### 2.3 Synthetic Scheme and Procedure

Compounds PS-1, PS-4, PS-6, PS-7, PS-8, PS-10, PS-11, PS-13, PS-14 and PS-18 were selected for further investigation due to their score in Pass online, Swiss ADME, Protox III, and molecular docking evaluations compared to other compounds.



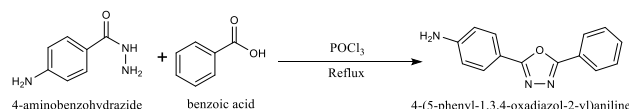
#### 2.3.1 Synthesis of 4-Aminobenzohydrazide from ethyl p-aminobenzoate

Ethyl p-aminobenzoate (0.1 mol) and  $\text{NH}_2\text{NH}_2 \cdot \text{H}_2\text{O}$  (0.2 mol) were refluxed in round bottom flask for 90 min. The reaction mixture was permitted to cool. The precipitate obtained was filtered and recrystallized from alcohol<sup>[41]</sup>.



#### 2.3.2 synthesis of (PS-1) 2-(4-amino phenyl) 5-phenyl 1,3,4-oxadiazole

Benzoic acid (0.5mole) and 4 amino benzo hydrazide (0.5mole) were placed in round bottom flask,  $\text{POCl}_3$  (1mole) was added dropwise to it and this mixture was refluxed for 30to40 min. It was permitted to reach room temperature. Water (15 ml) was added dropwise and then contents were refluxed for an additional 3 to 4 hours. The contents were permitted to cool to ambient temperature and were subsequently basified with a 0.1M KOH solution. The precipitate was filtered and recrystallized using ethanol. The reaction was monitored by thin-layer chromatography with Toluene: Ethyl Acetate: Acetic acid in a ratio of 7:3:1<sup>[42]</sup>.



Similarly other derivatives were prepared using relevant aromatic acids.

#### 2.3.3 Purity of Compound

Purity of synthesized 2(4-amino phenyl),5- substituted phenyl) 1,3,4-oxadiazoles was assessed using Merck HPTLC. Sample preparations were done in ethyl acetate strength 1mg/ml. Sample application was performed using a CAMAG Linomat 5 applicator tool on pre-coated silica gel 60 F<sub>254</sub> aluminium plates (size 10×10 cm), applying samples as bands. In optimized mobile phase of toluene: ethyl acetate: Acetic acid (7:3:1 v/v/v), which provided sharp, well-resolved bands and distinct R<sub>f</sub> values for all compounds<sup>[43-44]</sup>. Absorbance was measured at 273 nm. Mobile phase saturation time was 20 minutes with plate development time was 5 minutes.

#### 2.4 Nootropic Activity

The experimental protocol received approval from the IAEC of MGV's Pharmacy College, Panchavati, Nashik (Approval No. MGV/PC/CCSEA/XXXXI/01/2024-25/09).



### 2.4.1 Experimental Design

A total of 42 male Swiss-albino mice (4–6 weeks old, 15–20 g) were consumed in this study. They were accommodated under conventional conditions with a 7-day acclimatization period followed by a 7-day treatment period. The animals were be grouped into 7 groups (n=6). Group I served as the control as well as administered 0.1 ml of 0.5% CMC orally. Group II was administered scopolamine (1 mg/kg, i.p.) to induce memory destruction, serving as the negative control. Group III was treated with piracetam by i.p. (dose 200 mg/kg) as the standard nootropic active agent. Groups IV and V was treated with PS-1 at by p.o. with doses 200 and 400 mg/kg, respectively. Group VI was treated with PS-11 at 400 mg/kg p.o., and Group VII was treated with PS-14 at 400 mg/kg p.o. Doses were selected based on LD<sub>50</sub> values from the Protox-III database. Nootropic activity was evaluated using the Elevated Plus Maze and/or Morris Water Maze models, assessing both initial and retention transfer latencies.

### 2.4.2 Elevated Plus Maze Method:

To screen the effect of test compounds on memory and learning in Swiss albino mice the Elevated Plus Maze (EPM) method was utilized. It consisted of four arms—two open and two closed (each 30 cm × 5 cm)—connected by a central square (5 cm × 5 cm). The maze was elevated 50 cm above the floor. On the seventh day, following the administration of the designated doses, scopolamine was injected to induce amnesia. Forty-five minutes after scopolamine administration, the initial transfer latency (ITL) was recorded. ITL refers to the duration required for a mouse to transition from an open arm to one of the closed arms, with all four paws engaged. If a mouse failed to enter a closed arm within 90 seconds, it was gently guided into one, and the ITL was recorded as 90 seconds. Prior to ITL assessment, mice were trained to navigate the maze. Memory retention was assessed on the eighth day by measuring the retention transfer latency (RTL), which reflects the mouse's ability to recall the learned task. The inflexion ratio (IR) was calculated using the formula:  $IR = (L0 - L1) / L1$  Where: L0 = Initial Transfer Latency (seconds) L1 = Retention Transfer Latency (seconds) [45].

### 2.4.3 The Morris Water Maze Method (MWM):

The MWM technique was employed to evaluate memory in mice. The apparatus comprised a circular pool with a diameter of 60 cm and a height of 25 cm, containing 20 cm of water kept at a temperature of  $27 \pm 2^\circ\text{C}$ . The water was rendered opaque with a non-toxic white dye. The pool was partitioned into four equal quadrants by two threads positioned perpendicularly across the rim. A white platform measuring 6 cm by 6 cm was submerged 1 cm beneath the water surface in quadrant 4 (Q4), and its position remained unchanged during the training period. Each mouse was immersed in the water and allotted 120 seconds to identify the concealed platform. Mice participated in two trials daily, with a 20-minute inter-trial break, over a span of four consecutive days. Escape latency (EL)—the duration required to identify the concealed platform (maximum 90 seconds)—was documented for each trial. Upon locating the platform, a mouse was permitted to stay on it for 10 seconds. If it did not locate it within 90 seconds, it was softly directed to the platform and permitted to remain for 10 seconds before being extracted from the pool. A probe trial was undertaken after 24 hours, during which the platform was removed. The mouse was positioned in one of the remaining three quadrants and let to investigate the pool. The average duration spent in the target quadrant (Q4) searching for the absent platform was documented as an indicator of memory retention [46].

### 2.4.4 Statistical Analysis:

The GraphPad Prism 8 was utilized to analyse the results. The data from all experiments were expressed in the form of mean  $\pm$  SEM and analysed using ANOVA, followed by Dunnett's test for comparison. Values with  $p < 0.05$  were regarded as significant.

## 4. Results

### 4.1 In-silico evaluation for biological activity of designed molecules (pass online)

PASS online analysis revealed that all designed oxadiazole derivatives exhibited probable nootropic activity, with Pa values ranging from 0.356 to 0.590, while Pi values remained significantly lower. Compounds PS-1 (Pa = 0.584), PS-3 (0.590), PS-9 (0.566), PS-11 (0.547), PS-12 (0.577), and PS-14 (0.563) demonstrated comparatively higher Pa values, indicating a strong likelihood of nootropic potential (Table 1).



**Table 1: Predicted biological activities of the designed compounds using PASS online**

Compound	Biological activity (Predicted)	Pa	Pi
PS-1	Nootropic	0,584	0,084
PS-2	Nootropic	0,532	0,351
PS-3	Nootropic	0,590	0,081
PS-4	Nootropic	0,356	0,263
PS-5	Nootropic	0,515	0,121
PS-6	Nootropic	0,382	0,234
PS-7	Nootropic	0,536	0,109
PS-8	Nootropic	0,459	0,165
PS-9	Nootropic	0,566	0,093
PS-10	Nootropic	0,563	0,094
PS-11	Nootropic	0,547	0,102
PS-12	Nootropic	0,577	0,087
PS-13	Nootropic	0,374	0,242
PS-14	Nootropic	0,563	0,094
PS-15	Nootropic	0,533	0,111
PS-16	Nootropic	0,521	0,118
PS-17	Nootropic	0,541	0,106
PS-18	Nootropic	0,412	0,204
Piracetam	Nootropic	0,876	0,008

### 3.2 In silico evaluation for Pharmacokinetic properties of designed molecules. (SWISS ADME software)

SwissADME analysis indicated that most synthesized compounds exhibited acceptable drug-likeness profiles, with molecular weights within the permissible range for central nervous system (CNS) agents. Importantly, compounds PS-1, PS-4, PS-11, PS-14, and PS-16 were predicted to be blood–brain barrier (BBB) permeable, a critical prerequisite for nootropic drugs.(table 2&3).

**Table 2. ADME Prediction of synthesized compound by Swiss ADME Software.**

Comp. code	Mol.wt	Lipophilicity log o/w	Water solubility
PS-1	222	2.59	-3.38
PS-2	238.24	2.17	-3.23
PS-3	238.24	2.17	-3.23
PS-4	270.24	2.04	-3.01
PS-5	237.26	1.37	-2.19
PS-6	238.24	1.78	-3.06
PS-7	254.24	1.78	-3.06
PS-8	286.24	2.05	-3.12
PS-9	253.26	2.04	-3.23
PS-10	253.26	2.50	-3.23
PS-11	270.24	1.85	-3.28
PS-12	286.24	2.23	-3.12
PS-13	318.24	1.10	-2.82
PS-14	285.25	1.55	-2.91
PS-15	285.25	1.36	-2.91
PS-16	237.26	2.37	-3.38
PS-17	253.26	1.97	-3.23
PS-18	285.25	1.36	-2.91
Piracetam	142.16	0.79	-0.38

**Table 3. ADME Prediction of synthesized compound by Swiss ADME Software.**

Comp. code	GI Absorption	BBB	Bioavailability score
PS-1	+	Yes	0.55
PS-2	+	No	0.55
PS-3	+	No	0.55
PS-4	+	Yes	0.55
PS-5	+	No	0.55
PS-6	+	No	0.55



PS-7	+	No	0.55
PS-8	+	No	0.55
PS-9	+	No	0.55
PS-10	+	No	0.55
PS-11	+	Yes	0.55
PS-12	+	No	0.55
PS-13	-	No	0.55
PS-14	+	Yes	0.55
PS-15	+	No	0.55
PS-16	+	Yes	0.55
PS-17	+	No	0.55
PS-18	+	No	0.55
Piracetam	+	No	0.55

(-): Low; (+): High.

### 3.3 In silico pharmacological toxicity and dock score of designed molecules

Protox-III analysis predicted LD<sub>50</sub> values between 1260 and 2604 mg/kg, categorizing the compounds under low acute toxicity classes. Notably, PS-1, PS-11, and PS-14 showed favorable toxicity profiles with no predicted mutagenicity, immunotoxicity, or cytotoxicity, although mild hepatotoxicity was predicted for most compounds, a common observation for aromatic heterocycles (Table 4).

The superior docking performance of PS-1, PS-11, and PS-14 strongly correlated with their predicted BBB permeability and justified their selection for in vivo evaluation. Molecular docking studies against human acetylcholinesterase (PDB ID: 4PQE) demonstrated strong binding affinities for several oxadiazole derivatives (Table 4)

**Table 4. Toxicity profiles of designed derivative by Protox-III and Molecular Docking data**

Comp. code	Pr LD <sub>50</sub> (mg/kg)	Pr Accuracy %	H	C	I	M	u	Cy	Dock Score (Kcal/Mol)
PS-1	2000	72.9	A	A	I	I	I	I	-21
PS-2	2032	72.9	A	A	I	I	I	I	-19

PS-3	2000	72.9	A	A	I	I	I	-24
PS-4	2000	70.97	A	A	I	I	I	-5
PS-5	2412	69.26	A	A	I	I	I	-22
PS-6	2032	70.97	A	A	I	I	I	-22
PS-7	2300	69.26	A	A	I	I	I	-22
PS-8	1260	72.9	A	A	I	I	I	-21
PS-9	2000	70.97	A	A	I	I	I	-23
PS-10	2412	69.26	A	A	I	I	I	-18
PS-11	2412	69.26	A	A	I	I	A	-23
PS-12	2604	69.26	A	A	I	I	A	-22
PS-13	2000	69.26	A	A	I	I	I	-9
PS-14	2500	69.26	A	A	I	I	I	-25
PS-15	2500	69.26	A	A	I	I	I	-22
PS-16	2500	70.97	A	A	I	I	I	-23
PS-17	2000	70.97	A	A	I	I	I	-21
PS-18	2032	70.90	A	A	I	I	I	-22
Piracetam	2000	100	I	I	I	I	I	-21

Pr: Predicted, H: Hepatotoxicity, C: Carcinogenicity, Im: Immunotoxicity, Mu: Mutagenicity, Cy: Cytotoxicity

A: Active; I: Inactive

### 3.4 Molecular Docking using Molecular Modeling

Using Biovia Software 2Dimensional and 3Dimensional images of ligands with protein were analyzed for active sites. 2D and 3 D images of PS 14 with protein can be shown in figure 3a and figure 3b.

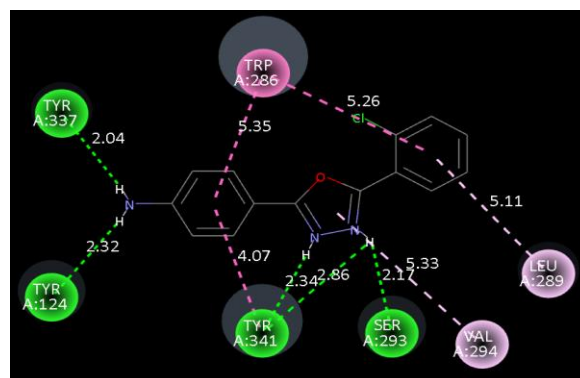


**Figure 3a. 2D molecular visualization of PS 14 and protein Biovia software**

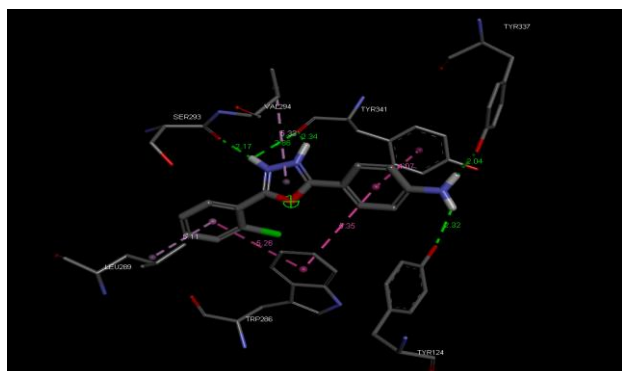


**Figure 3b. 3D molecular visualization of PS-14 with protein using Biovia software**

Ten selected derivatives were successfully synthesized using a  $\text{POCl}_3$ -mediated cyclization approach. The reactions proceeded smoothly with moderate to good yields, and structures were confirmed using IR and  $^1\text{H}$  NMR spectroscopy.

Characteristic IR peaks corresponding to  $\text{C}=\text{N}$  stretching of the oxadiazole ring ( $1680\text{--}1705\text{ cm}^{-1}$ ) and  $\text{N-H}$  stretching ( $3300\text{--}3450\text{ cm}^{-1}$ ) confirmed successful ring closure.  $^1\text{H}$  NMR spectra displayed appropriate aromatic proton signals and amine protons, consistent with the proposed structures. These findings validated the structural integrity of the synthesized compounds.

### 5. Spectral characterization of optimized compounds.

PS-1 -  $\text{C}_{14}\text{H}_{11}\text{N}_3\text{O}$  (237.26). Appearance: white solid, melting point  $131\text{ }^\circ\text{C}$ . IR:  $3429.78\text{ cm}^{-1}$  ( $\text{N-H}$  stretch),  $3033.48\text{ cm}^{-1}$  ( $\text{Ar-H}$  stretch),  $1681.62\text{ cm}^{-1}$  ( $\text{C}=\text{N}$ , oxadiazole),  $1626.66\text{ cm}^{-1}$  ( $\text{N-H}$  bending),  $1171.54\text{ cm}^{-1}$  ( $\text{C-O}$ , oxadiazole),  $842.74\text{ cm}^{-1}$  ( $\text{Ar-H}$  bending).  $^1\text{H}$  NMR ( $\delta$ , ppm):  $10.58$  (2H, broad singlet,  $-\text{NH}_2$ ),  $7.96$  (2H, doublet, aromatic CH),  $7.63$  (1H, triplet, aromatic CH),  $7.52$  (2H, doublet, aromatic CH),  $6.53$  (2H, doublet, aromatic CH).

PS-11 -  $\text{C}_{15}\text{H}_{13}\text{N}_3\text{O}_3$  (283.28). Brown solid, melting point  $140\text{ }^\circ\text{C}$ . IR:  $3306.82\text{ cm}^{-1}$  ( $\text{N-H}$  stretch),  $3033.48\text{ cm}^{-1}$  ( $\text{O-H}$ ),  $3059.3\text{ cm}^{-1}$  ( $\text{Ar-H}$ ),  $1697.19\text{ cm}^{-1}$  ( $\text{C}=\text{N}$ ),  $1630\text{ cm}^{-1}$  ( $\text{N-H}$  bending),  $1174\text{ cm}^{-1}$  ( $\text{C-O}$ ),  $770.423\text{ cm}^{-1}$  ( $\text{Ar-H}$  bending).  $^1\text{H}$  NMR ( $\delta$ , ppm):  $6.79$  (2H, ddd),  $7.23$  (1H, doublet),  $7.34\text{--}7.62$  (6H, aromatic),  $7.70$  (2H, ddd).

PS-14 -  $\text{C}_{14}\text{H}_{10}\text{ClN}_3\text{O}$  (271.70). White solid, melting point  $151\text{ }^\circ\text{C}$ . IR:  $3347.82\text{ cm}^{-1}$  ( $\text{N-H}$  stretch),  $3065.3\text{ cm}^{-1}$  ( $\text{Ar-H}$  stretch),  $1693.19\text{ cm}^{-1}$  ( $\text{C}=\text{N}$ ),  $1279.54\text{ cm}^{-1}$

( $\text{C-O}$ ),  $770.423\text{ cm}^{-1}$  ( $\text{Ar-H}$  bending),  $696.177\text{ cm}^{-1}$  ( $\text{C-Cl}$  stretch).  $^1\text{H}$  NMR ( $\delta$ , ppm):  $6.60$  (2H, singlet,  $-\text{NH}_2$ ),  $7.10$  (1H, doublet),  $6.80$  (2H, doublet),  $7.40$  (1H, triplet),  $7.60$  (2H, doublet),  $7.20$  (2H, doublet).

### 3.5 Purity analysis of compound by HPTLC

HPTLC analysis demonstrated excellent purity of the lead compounds. PS-11 and PS-14 showed 100% purity, while PS-1 exhibited 99.05% purity, confirming the absence of significant impurities. Sharp, well-resolved peaks and consistent  $R_f$  values further established the reliability of the synthesis and purification methods (as shown in figure 4 and table 5).

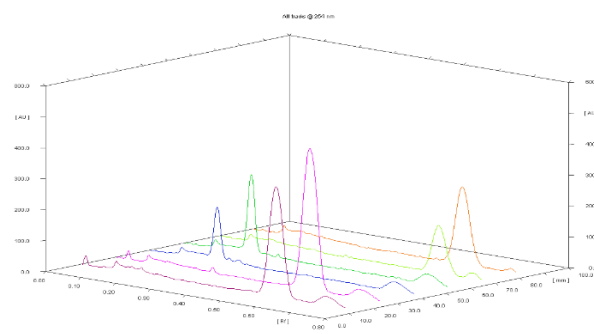


**Figure 4. 3D Surface Plot of compound PS-1, PS-11, PS-14**

**Table 5: HPTLC Analysis:  $R_f$ , Area, and Purity Assessment of Synthesized Compound**

S. No	Compound Code	$R_f$ value	Area	Observation of % Purity
1.	PS-1 Pure Comp	0.28	14030.9	99.05 %
	PS-1 Impurity	0.56	134.2	0.95 %
2.	PS-11	0.19	3749.7	100 %
3.	PS-14	0.60	7568.4	100 %

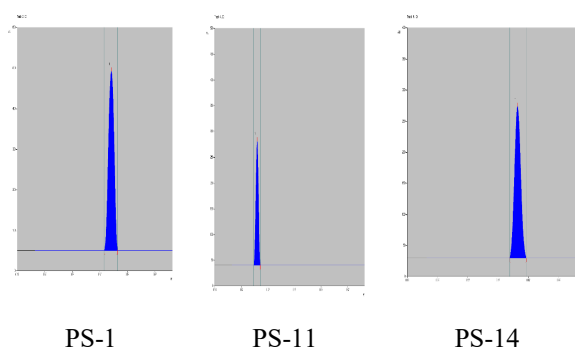
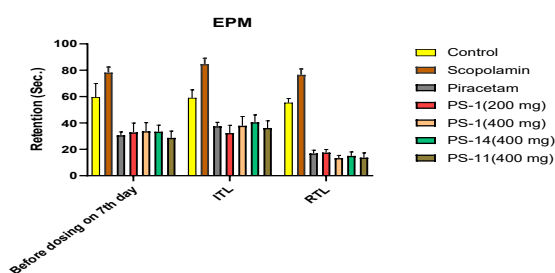


**Figure 6.** Densitogram of compound PS-1, PS-11, and PS-14

### 3.5 Nootropic Activity

#### 3.5.1 Elevated Plus Maze

In the scopolamine-induced amnesia model, scopolamine significantly increased both initial transfer latency (ITL) and retention transfer latency (RTL), confirming memory impairment. Treatment with PS-1, PS-11, and PS-14 significantly reduced ITL and RTL values ( $p < 0.0001$ ), indicating effective reversal of amnesia (Figure 7).



The values are expressed as mean  $\pm$  SEM ( $n=6$ ), [ns = Not significant, \*\*\*\* =  $p < 0.0001$ ]

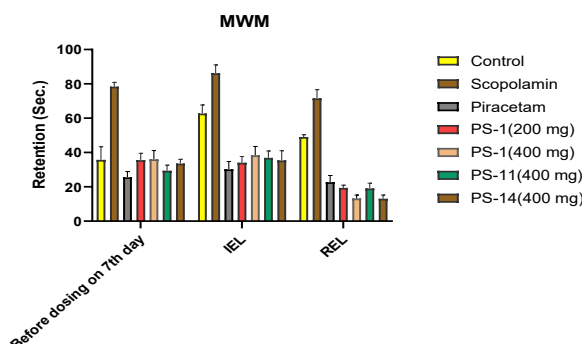
**Figure 7.** Graphical representation of Elevated Plus Maze activity

#### 3.5.2 Morris Water Maze model

In the Morris Water Maze test, scopolamine-treated animals exhibited prolonged escape latency and reduced time spent in the target quadrant, reflecting impaired spatial memory. Administration of PS-1, PS-11, and PS-14 significantly reduced escape latency and increased target quadrant exploration during the probe trial.

PS-14 at 400 mg/kg demonstrated the most pronounced improvement, closely paralleling its superior docking score and BBB permeability (Figure 8). These results

suggest that the synthesized oxadiazoles effectively enhance both learning acquisition and memory retention.



The values are expressed as mean  $\pm$  SEM ( $n=6$ ), [ns = Not significant, \*\*\*\* =  $p < 0.0001$ ]

**Figure 8.** Graphical representation of Morris Water Maze Mode

### 5. Discussion

The present study aimed to identify novel nootropic agents based on the 1,3,4-oxadiazole scaffold through a sequential workflow involving in-silico screening, chemical synthesis, spectral characterization, purity assessment, and in-vivo pharmacological evaluation. A total of eighteen designed derivatives (PS-1 to PS-18) were initially evaluated computationally, of which ten compounds were synthesized and three lead molecules (PS-1, PS-11, and PS-14) were selected for detailed biological evaluation. Although the  $P_a$  values of the synthesized compounds were lower than that of the standard drug piracetam ( $P_a = 0.876$ ), PASS predictions primarily provide qualitative probability rather than quantitative efficacy. The favorable  $P_a > P_i$  relationship across the series justified further pharmacokinetic and docking investigations. All tested compounds showed high gastrointestinal absorption and a uniform bioavailability score of 0.55, comparable to piracetam. The lipophilicity (LogP 1.1–2.6) suggested an optimal balance between aqueous solubility and membrane permeability, facilitating CNS penetration without excessive nonspecific tissue binding. These findings supported the suitability of selected compounds for in vivo evaluation. From toxicity study it revealed that compared to piracetam, which displayed complete inactivity across all toxicity endpoints, the synthesized oxadiazoles still remained within acceptable safety margins, enabling dose selection for animal studies.



Docking scores ranged from -18 to -25 kcal/mol, with PS-14 exhibiting the highest binding affinity (-25 kcal/mol), surpassing piracetam (-21 kcal/mol).

Key interactions were observed with crucial residues involved in AChE inhibition, particularly TRP286, TYR341, SER293, TYR124, and VAL294. The presence of  $\pi$ - $\pi$  stacking interactions with TRP286, a residue essential for enzyme inhibition, suggests a stable ligand-enzyme complex and supports a cholinesterase inhibitory mechanism. In pharmacological activity evaluation it observed that at 400 mg/kg, PS-1 and PS-11 exhibited performance comparable to piracetam, while PS-14 showed slightly superior retention improvement. The calculated inflexion ratios further confirmed enhanced memory consolidation.

The observed nootropic activity appears strongly influenced by phenyl substitution patterns on the oxadiazole ring. Electron-donating and moderately lipophilic substituents enhanced AChE binding, BBB penetration, and in vivo efficacy. Particularly, the chloro-substituted PS-14 exhibited optimal balance between lipophilicity and receptor interaction, explaining its superior performance.

## 6. conclusion

The present study successfully demonstrated the potential of 2-(4-aminophenyl), 5-substituted phenyl-1,3,4-oxadiazole derivatives as promising nootropic agents through a systematic approach involving rational design, in-silico screening, chemical synthesis, and in-vivo pharmacological evaluation. A library of eighteen novel oxadiazole derivatives was initially designed and subjected to computational evaluation, which enabled the identification of lead candidates with favorable biological activity, pharmacokinetic properties, blood-brain barrier permeability, and acceptable safety profiles.

Molecular docking studies using Molsoft ICM-Pro revealed that several compounds exhibited strong binding affinity toward acetylcholinesterase, with docking scores comparable to or better than the standard drug piracetam. Among them, PS-14 showed the highest binding affinity, followed by PS-3, PS-9, PS-11, and PS-16, indicating effective interaction with key amino acid residues involved in enzyme inhibition. These findings strongly support the cholinesterase inhibitory mechanism as a probable mode of nootropic action.

Based on in-silico predictions, ten compounds were synthesized and structurally confirmed by IR and <sup>1</sup>H-NMR spectroscopy. High purity of the lead compounds was further established through HPTLC analysis. In-vivo evaluation using scopolamine-induced amnesia models, including the Elevated Plus Maze and Morris Water Maze, demonstrated that PS-1, PS-11, and PS-14 significantly improved learning and memory parameters at both tested doses, with effects comparable to piracetam. The dose-dependent cognitive enhancement observed confirms their efficacy as nootropic agents.

Overall, the study establishes 1,3,4-oxadiazole as a valuable heterocyclic scaffold for the development of novel nootropic agents. The consistency observed between in-silico docking results, pharmacokinetic predictions, and in-vivo behavioral outcomes validates the rational drug design strategy employed. These findings suggest that the identified lead compounds, particularly PS-14, warrant further investigation, including detailed mechanistic studies and advanced preclinical evaluation, to explore their full therapeutic potential in the management of AD and other cognitive disorders.

## 7. Acknowledgement

Authors are very thankful to Dr. R.S. Bhambar, Principal, MG V's pharmacy college Panchavati, Nasik - 03 and management for providing facilities to carry out mentioned research work.

## 8. Conflict of Interest

None

## 9. References

- [1]. Tahami M.A., Byrnes M. J., White L. A., Zhang Q., 2022. Alzheimer's disease: epidemiology and clinical progression. *Neurology and therapy*. Jun;11(2),553-69.
- [2]. Abubakar M.B., Sanusi K.O., Ugusman A., Mohamed W., Kamal H., Ibrahim N.H., et al., 2022. Alzheimer's disease: an update and insights into pathophysiology. *Frontiers in aging neuroscience*. Mar 30(14), 742408.
- [3]. Tiwari S., Atluri V., Kaushik A., Yndart A., Nair M., 2019. Alzheimer's disease: pathogenesis, diagnostics, and therapeutics.



- International journal of nanomedicine. Jul 19, 5541-54.
- [4]. Duyckaerts C., Dickson D., 2011. Neuropathology of Alzheimer's disease and its variants. *Neurodegeneration: the molecular pathology of dementia and movement disorders*. Sep 2, 62-91.
- [5]. Duyckaerts C., Delatour B., Potier M.C., 2009. Classification and basic pathology of Alzheimer disease. *Acta neuropathologica*. 118(1), 5-36.
- [6]. Frings L., Spehl T. S., Weber W. A., Hüll M., Meyer P.T., 2013. Amyloid- $\beta$  load predicts medial temporal lobe dysfunction in Alzheimer dementia. *Journal of Nuclear Medicine*. 54(11), 1909-14.
- [7]. Shinohara M., Koga S., Konno T., Nix J., Shinohara M., Aoki N., et al., 2017. Distinct spatiotemporal accumulation of N-truncated and full-length amyloid- $\beta$ 42 in Alzheimer's disease. *Brain*. 140(12), 3301-16.
- [8]. Rahman A., Jaiswal A., Keshari P., Singh DK., Alzheimer's: Epidemiology, Pathophysiology, Diagnosis, and Treatments. In *Proteostasis: Investigating Molecular Dynamics in Neurodegenerative Disorders*. Singapore: Springer Nature Singapore, 2025 Jul 13 (pp. 39-72).
- [9]. Liu S., Geng D., 2025. A systematic analysis for disease burden, risk factors, and trend projection of Alzheimer's disease and other dementias in China and globally. *PLoS One*. May 7;20(5), e0322574.
- [10]. Pepeu G., Spignoli G., 1989. Nootropic drugs and brain cholinergic mechanisms. *Progress in Neuro-Psychopharmacology and Biological Psychiatry*. 13(1), S77-88.
- [11]. Joshi P. C., 2013. A review on natural memory enhancers (Nootropics). *Unique Journal of Engineering and Advanced Sciences*. 1(01), 8-18.
- [12]. Sheppard O., Coleman M., Alzheimer's disease: etiology, neuropathology and pathogenesis. Exon Publications: Australia, 2020.
- [13]. Zawia NH, Basha MR. Environmental risk factors and the developmental basis for Alzheimer's disease. *Reviews in the Neurosciences*. 2005 Aug;16(4):325-38.
- [14]. Ghersi-Egea J.F., Gorevic P.D., Ghiso J., Frangione B., Patlak C.S., Fenstermacher J.D., 1996. Fate of cerebrospinal fluid-borne amyloid  $\beta$ -peptide: rapid clearance into blood and appreciable accumulation by cerebral arteries. *Journal of neurochemistry*. 67(2), 880-3.
- [15]. Weller R.O., Subash M., Preston S.D., Mazanti I., Carare R.O., Symposium: 2008. clearance of A $\beta$  from the brain in Alzheimer's disease: perivascular drainage of amyloid- $\beta$  peptides from the brain and its failure in cerebral amyloid angiopathy and Alzheimer's disease. *Brain Pathology*. 18(2), 253-66.
- [16]. Preston S.D., Steart P.V., Wilkinson A., Nicoll J.A., Weller R.O., 2003. Capillary and arterial cerebral amyloid angiopathy in Alzheimer's disease: defining the perivascular route for the elimination of amyloid  $\beta$  from the human brain. *Neuropathology and applied neurobiology*. 29(2), 106-17.
- [17]. Alonso A.D., Inge G.I., Barra H.S., Iqbal K., 1997. Abnormal phosphorylation of tau and the mechanism of Alzheimer neurofibrillary degeneration: sequestration of microtubule-associated proteins 1 and 2 and the disassembly of microtubules by the abnormal tau. *Neuroscience*. 94(1), 298-303.
- [18]. Cowan C.M., Bossing T., Page A., Shepherd D., Mudher A., 2010. Soluble hyperphosphorylated tau causes microtubule breakdown and functionally compromises normal tau in vivo. *Acta neuropathologica*. 20(5), 593-604.
- [19]. Billingsley M.L., Kincaid R.L., 1997. Regulated phosphorylation and dephosphorylation of tau protein: effects on microtubule interaction, intracellular trafficking and neurodegeneration. *Biochemical Journal*. 323(3), 577-91.
- [20]. Spires-Jones T.L., Hyman B.T., 2014. The intersection of amyloid beta and tau at synapses in Alzheimer's disease. *Neuron*. 82(4), 756-71.
- [21]. Rajmohan R., Reddy P.H., 2017. Amyloid-beta and phosphorylated tau accumulations cause abnormalities at synapses of Alzheimer's



- disease neurons. *Journal of Alzheimer's Disease*. 57(4), 975-99.
- [22]. Perry E.K., 1988. Acetylcholine and Alzheimer's disease. *The British Journal of Psychiatry*. 152(6), 737-40.
- [23]. Terry A.V., Buccafusco J.J., 2003. The cholinergic hypothesis of age and Alzheimer's disease-related cognitive deficits: recent challenges and their implications for novel drug development. *The Journal of pharmacology and experimental therapeutics*. 306(3), 821-7.
- [24]. Cacabelos R., Martínez I. O, Cacabelos N., Carrera I., Corzo L., Naidoo V., 2024. Therapeutic options in Alzheimer's disease: from classic acetylcholinesterase inhibitors to multi-target drugs with pleiotropic activity. *Life*. 14(12), 1555.
- [25]. Froestl W., Muhs A., Pfeifer A., 2013. Cognitive enhancers (nootropics). Part 2: Drugs interacting with enzymes. *Journal of Alzheimer's Disease*. 33(3), 547-658.
- [26]. Vaidya A., Jain S., Jain P., Jain P., Tiwari N., Jain R., et al., 2016. Synthesis and biological activities of oxadiazole derivatives: A review. *Mini reviews in medicinal chemistry*. 6(10), 825-45.
- [27]. Mohan M., Rathinasamy G., Devarajan B., Byran G., Lakshmanan K. A., 2025. Pharmacological Update of Oxadiazole Derivatives: A Review. *Current Topics in Medicinal Chemistry*. 25(20), 2367-84.
- [28]. Gujjarappa R., et al. 2022. An Overview on Biological Activities of Oxazole, Isoxazoles and 1,2,4-Oxadiazoles Derivatives. In: Swain, B.P. (eds) *Nanostructured Biomaterials. Materials Horizons: From Nature to Nanomaterials*. Springer, Singapore.
- [29]. Voronina T.A., 2023. Cognitive impairment and nootropic drugs: mechanism of action and spectrum of effects. *Neurochemical journal*. 7(2), 180-8.
- [30]. Lerner P.P., Miodownik C., Lerner V., 2015. Tardive dyskinesia (syndrome): current concept and modern approaches to its management. *Psychiatry and clinical neurosciences*. 69(6), 321-34.
- [31]. Katti S.A., Revar N., Sonawane S., Pawar S.N., Patil R.A., et al., 2024. Design, Synthesis and In-silico Evaluation of 1,3,4 Oxadiazole derivatives for their Nootropic Activity. *Chettinad Health City Medical Journal*. 13(4), 43-54.
- [32]. Lagunin A., Stepanchikova A., Filimonov D., Poroikov V., 2000. PASS: prediction of activity spectra for biologically active substances. *Bioinformatics*. 16(8), 747-8.
- [33]. Daina A., Zoete V., 2019. Application of the Swiss Drug Design Online Resources in Virtual Screening. *Int J Mol Sci*. 20(18), 4612.
- [34]. Banerjee P., Kemmler E., Dunkel M., Preissner R., 2024. ProTox 3.0: a webserver for the prediction of toxicity of chemicals. *Nucleic Acids Res*. 52(W1), W513-20.
- [35]. Yang C., Chen E.A., Zhang Y., 2022. Protein-Ligand Docking in the Machine-Learning Era. *Molecules*. 27(14), 4568.
- [36]. Berman H.M., 2000. The Protein Data Bank. *Nucleic Acids Res*. 28(1), 235-42.
- [37]. Abagyan R., Totrov M., Kuznetsov D., 1994. ICM—A new method for protein modeling and design: Applications to docking and structure prediction from the distorted native conformation. *J Comput Chem*. 5(5), 488-506.
- [38]. Sussman J.L., Harel M., Frolow F., Oefner C., Goldman A., Toker L., et al. 1991. Atomic Structure of Acetylcholinesterase from *Torpedo californica*: A Prototypic Acetylcholine-Binding Protein. *Science*. 253(5022), 872-9.
- [39]. Khare N., Maheshwari S.K., Jha A.K., 2021. Screening and identification of secondary metabolites in the bark of *Bauhinia variegata* to treat Alzheimer's disease by using molecular docking and molecular dynamics simulations. *J Biomol Struct Dyn*. 39(16):5988-98.
- [40]. Sedaghat A., Rezaee E., Hosseini O., Tabatabai S.A., 2020. Para-Aminobenzohydrazide Derivatives as Fatty Acid Amide Hydrolase Inhibitors: Design, Synthesis and Biological Evaluation. *Iran J Pharm Res*. 19(4), 103-112.



---

<https://doi.org/10.22037/ijpr.2020.113899.145>

51

- [41]. Makwana H., Naliapara Y.T.,2014. Synthesis, Characterization and Biological Evaluation of 2,5-di-Substituted 1,3,4-Oxadiazole Derivatives. *Int Lett Chem Phys Astron.* 34,48–54.
- [42]. Bagul M., Srinivasa H., Padh H., Rajani M.,2005. A rapid densitometric method for simultaneous quantification of gallic acid and ellagic acid in herbal raw materials using HPTLC. *J Sep Sci.* 28(6),581–4.
- [43]. Dhalwal K., Shinde V.M., Biradar Y.S., Mahadik K.R.,2008. Simultaneous quantification of bergenin, catechin, and gallic acid from *Bergenia ciliata* and *Bergenia ligulata* by using thin-layer chromatography. *Journal of food composition and analysis.* 21(6),496-500.
- [44]. Sharma A.C., Kulkarni S.K.,1992. Evaluation of learning and memory mechanisms employing elevated plus-maze in rats and mice. *Prog Neuropsychopharmacol Biol Psychiatry.* 16(1),117–25.
- [45]. Vorhees C.V., Williams M.T.,2006. Morris water maze: procedures for assessing spatial and related forms of learning and memory. *Nat Protoc.* 1(2),848–58.